BABAR-CONF-01/23
SLAC-PUB-8913
July, 2001

Measurement of the $B^0\overline{B}^0$ Oscillation Frequency in Hadronic B^0 Decays

The *BABAR* Collaboration

July 11, 2001

Abstract

$B^0\overline{B}^0$ flavor oscillations have been studied in 20.7 fb^{-1} of e^+e^- annihilation data collected in 1999 and 2000 with the *BABAR* detector at center-of-mass energies near the $\Upsilon(4S)$ resonance. The event sample consists of one B^0 meson fully reconstructed in a hadronic decay mode, while the flavor of the recoiling B^0 in the event is determined with a tagging algorithm that exploits the correlation between the flavor of the heavy quark and the charges of its decay products. By fitting the time development of the observed mixed and unmixed final states, the $B^0\overline{B}^0$ oscillation frequency, Δm_d, is determined to be $0.519 \pm 0.020 \pm 0.016\,\hbar\,\mathrm{ps}^{-1}$.

Submitted to the International Europhysics Conference on High Energy Physics,
7/12—7/18/2001, Budapest, Hungary

Stanford Linear Accelerator Center, Stanford University, Stanford, CA 94309

Work supported in part by Department of Energy contract DE-AC03-76SF00515.

The *BABAR* Collaboration,

B. Aubert, D. Boutigny, J.-M. Gaillard, A. Hicheur, Y. Karyotakis, J. P. Lees, P. Robbe, V. Tisserand

Laboratoire de Physique des Particules, F-74941 Annecy-le-Vieux, France

A. Palano

Università di Bari, Dipartimento di Fisica and INFN, I-70126 Bari, Italy

G. P. Chen, J. C. Chen, N. D. Qi, G. Rong, P. Wang, Y. S. Zhu

Institute of High Energy Physics, Beijing 100039, China

G. Eigen, P. L. Reinertsen, B. Stugu

University of Bergen, Inst. of Physics, N-5007 Bergen, Norway

B. Abbott, G. S. Abrams, A. W. Borgland, A. B. Breon, D. N. Brown, J. Button-Shafer, R. N. Cahn, A. R. Clark, M. S. Gill, A. V. Gritsan, Y. Groysman, R. G. Jacobsen, R. W. Kadel, J. Kadyk, L. T. Kerth, S. Kluth, Yu. G. Kolomensky, J. F. Kral, C. LeClerc, M. E. Levi, T. Liu, G. Lynch, A. B. Meyer, M. Momayezi, P. J. Oddone, A. Perazzo, M. Pripstein, N. A. Roe, A. Romosan, M. T. Ronan, V. G. Shelkov, A. V. Telnov, W. A. Wenzel

Lawrence Berkeley National Laboratory and University of California, Berkeley, CA 94720, USA

P. G. Bright-Thomas, T. J. Harrison, C. M. Hawkes, D. J. Knowles, S. W. O'Neale, R. C. Penny, A. T. Watson, N. K. Watson

University of Birmingham, Birmingham, B15 2TT, United Kingdom

T. Deppermann, K. Goetzen, H. Koch, J. Krug, M. Kunze, B. Lewandowski, K. Peters, H. Schmuecker, M. Steinke

Ruhr Universität Bochum, Institut für Experimentalphysik 1, D-44780 Bochum, Germany

J. C. Andress, N. R. Barlow, W. Bhimji, N. Chevalier, P. J. Clark, W. N. Cottingham, N. De Groot, N. Dyce, B. Foster, J. D. McFall, D. Wallom, F. F. Wilson

University of Bristol, Bristol BS8 1TL, United Kingdom

K. Abe, C. Hearty, T. S. Mattison, J. A. McKenna, D. Thiessen

University of British Columbia, Vancouver, BC, Canada V6T 1Z1

S. Jolly, A. K. McKemey, J. Tinslay

Brunel University, Uxbridge, Middlesex UB8 3PH, United Kingdom

V. E. Blinov, A. D. Bukin, D. A. Bukin, A. R. Buzykaev, V. B. Golubev, V. N. Ivanchenko, A. A. Korol, E. A. Kravchenko, A. P. Onuchin, A. A. Salnikov, S. I. Serednyakov, Yu. I. Skovpen, V. I. Telnov, A. N. Yushkov

Budker Institute of Nuclear Physics, Novosibirsk 630090, Russia

D. Best, A. J. Lankford, M. Mandelkern, S. McMahon, D. P. Stoker

University of California at Irvine, Irvine, CA 92697, USA

A. Ahsan, K. Arisaka, C. Buchanan, S. Chun

University of California at Los Angeles, Los Angeles, CA 90024, USA

J. G. Branson, D. B. MacFarlane, S. Prell, Sh. Rahatlou, G. Raven, V. Sharma

University of California at San Diego, La Jolla, CA 92093, USA

C. Campagnari, B. Dahmes, P. A. Hart, N. Kuznetsova, S. L. Levy, O. Long, A. Lu, J. D. Richman, W. Verkerke, M. Witherell, S. Yellin

University of California at Santa Barbara, Santa Barbara, CA 93106, USA

J. Beringer, D. E. Dorfan, A. M. Eisner, A. Frey, A. A. Grillo, M. Grothe, C. A. Heusch, R. P. Johnson, W. Kroeger, W. S. Lockman, T. Pulliam, H. Sadrozinski, T. Schalk, R. E. Schmitz, B. A. Schumm, A. Seiden, M. Turri, W. Walkowiak, D. C. Williams, M. G. Wilson

University of California at Santa Cruz, Institute for Particle Physics, Santa Cruz, CA 95064, USA

E. Chen, G. P. Dubois-Felsmann, A. Dvoretskii, D. G. Hitlin, S. Metzler, J. Oyang, F. C. Porter, A. Ryd, A. Samuel, M. Weaver, S. Yang, R. Y. Zhu

California Institute of Technology, Pasadena, CA 91125, USA

S. Devmal, T. L. Geld, S. Jayatilleke, G. Mancinelli, B. T. Meadows, M. D. Sokoloff

University of Cincinnati, Cincinnati, OH 45221, USA

T. Barillari, P. Bloom, M. O. Dima, S. Fahey, W. T. Ford, D. R. Johnson, U. Nauenberg, A. Olivas, H. Park, P. Rankin, J. Roy, S. Sen, J. G. Smith, W. C. van Hoek, D. L. Wagner

University of Colorado, Boulder, CO 80309, USA

J. Blouw, J. L. Harton, M. Krishnamurthy, A. Soffer, W. H. Toki, R. J. Wilson, J. Zhang

Colorado State University, Fort Collins, CO 80523, USA

T. Brandt, J. Brose, T. Colberg, G. Dahlinger, M. Dickopp, R. S. Dubitzky, A. Hauke, E. Maly, R. Müller-Pfefferkorn, S. Otto, K. R. Schubert, R. Schwierz, B. Spaan, L. Wilden

Technische Universität Dresden, Institut für Kern- und Teilchenphysik, D-01062, Dresden, Germany

L. Behr, D. Bernard, G. R. Bonneaud, F. Brochard, J. Cohen-Tanugi, S. Ferrag, E. Roussot, S. T'Jampens, Ch. Thiebaux, G. Vasileiadis, M. Verderi

Ecole Polytechnique, F-91128 Palaiseau, France

A. Anjomshoaa, R. Bernet, A. Khan, D. Lavin, F. Muheim, S. Playfer, J. E. Swain

University of Edinburgh, Edinburgh EH9 3JZ, United Kingdom

M. Falbo

Elon University, Elon University, NC 27244-2010, USA

C. Borean, C. Bozzi, S. Dittongo, M. Folegani, L. Piemontese

Università di Ferrara, Dipartimento di Fisica and INFN, I-44100 Ferrara, Italy

E. Treadwell

Florida A&M University, Tallahassee, FL 32307, USA

F. Anulli,[1] R. Baldini-Ferroli, A. Calcaterra, R. de Sangro, D. Falciai, G. Finocchiaro, P. Patteri, I. M. Peruzzi,[2]1 M. Piccolo, Y. Xie, A. Zallo

Laboratori Nazionali di Frascati dell'INFN, I-00044 Frascati, Italy

[1] Also with Università di Perugia, I-06100 Perugia, Italy

S. Bagnasco, A. Buzzo, R. Contri, G. Crosetti, P. Fabbricatore, S. Farinon, M. Lo Vetere, M. Macri, M. R. Monge, R. Musenich, M. Pallavicini, R. Parodi, S. Passaggio, F. C. Pastore, C. Patrignani, M. G. Pia, C. Priano, E. Robutti, A. Santroni

Università di Genova, Dipartimento di Fisica and INFN, I-16146 Genova, Italy

M. Morii

Harvard University, Cambridge, MA 02138, USA

R. Bartoldus, T. Dignan, R. Hamilton, U. Mallik

University of Iowa, Iowa City, IA 52242, USA

J. Cochran, H. B. Crawley, P.-A. Fischer, J. Lamsa, W. T. Meyer, E. I. Rosenberg

Iowa State University, Ames, IA 50011-3160, USA

M. Benkebil, G. Grosdidier, C. Hast, A. Höcker, H. M. Lacker, S. Laplace, V. Lepeltier, A. M. Lutz, S. Plaszczynski, M. H. Schune, S. Trincaz-Duvoid, A. Valassi, G. Wormser

Laboratoire de l'Accélérateur Linéaire, F-91898 Orsay, France

R. M. Bionta, V. Brigljević , D. J. Lange, M. Mugge, X. Shi, K. van Bibber, T. J. Wenaus, D. M. Wright, C. R. Wuest

Lawrence Livermore National Laboratory, Livermore, CA 94550, USA

M. Carroll, J. R. Fry, E. Gabathuler, R. Gamet, M. George, M. Kay, D. J. Payne, R. J. Sloane, C. Touramanis

University of Liverpool, Liverpool L69 3BX, United Kingdom

M. L. Aspinwall, D. A. Bowerman, P. D. Dauncey, U. Egede, I. Eschrich, N. J. W. Gunawardane, J. A. Nash, P. Sanders, D. Smith

University of London, Imperial College, London, SW7 2BW, United Kingdom

D. E. Azzopardi, J. J. Back, P. Dixon, P. F. Harrison, R. J. L. Potter, H. W. Shorthouse, P. Strother, P. B. Vidal, M. I. Williams

Queen Mary, University of London, E1 4NS, United Kingdom

G. Cowan, S. George, M. G. Green, A. Kurup, C. E. Marker, P. McGrath, T. R. McMahon, S. Ricciardi, F. Salvatore, I. Scott, G. Vaitsas

University of London, Royal Holloway and Bedford New College, Egham, Surrey TW20 0EX, United Kingdom

D. Brown, C. L. Davis

University of Louisville, Louisville, KY 40292, USA

J. Allison, R. J. Barlow, J. T. Boyd, A. C. Forti, J. Fullwood, F. Jackson, G. D. Lafferty, N. Savvas, E. T. Simopoulos, J. H. Weatherall

University of Manchester, Manchester M13 9PL, United Kingdom

A. Farbin, A. Jawahery, V. Lillard, J. Olsen, D. A. Roberts, J. R. Schieck

University of Maryland, College Park, MD 20742, USA

G. Blaylock, C. Dallapiccola, K. T. Flood, S. S. Hertzbach, R. Kofler, T. B. Moore, H. Staengle, S. Willocq

University of Massachusetts, Amherst, MA 01003, USA

B. Brau, R. Cowan, G. Sciolla, F. Taylor, R. K. Yamamoto
Massachusetts Institute of Technology, Laboratory for Nuclear Science, Cambridge, MA 02139, USA

M. Milek, P. M. Patel, J. Trischuk
McGill University, Montréal, Canada QC H3A 2T8

F. Lanni, F. Palombo
Università di Milano, Dipartimento di Fisica and INFN, I-20133 Milano, Italy

J. M. Bauer, M. Booke, L. Cremaldi, V. Eschenburg, R. Kroeger, J. Reidy, D. A. Sanders, D. J. Summers
University of Mississippi, University, MS 38677, USA

J. P. Martin, J. Y. Nief, R. Seitz, P. Taras, A. Woch, V. Zacek
Université de Montréal, Laboratoire René J. A. Lévesque, Montréal, Canada QC H3C 3J7

H. Nicholson, C. S. Sutton
Mount Holyoke College, South Hadley, MA 01075, USA

C. Cartaro, N. Cavallo,[3] G. De Nardo, F. Fabozzi, C. Gatto, L. Lista, P. Paolucci, D. Piccolo, C. Sciacca
Università di Napoli Federico II, Dipartimento di Scienze Fisiche and INFN, I-80126, Napoli, Italy

J. M. LoSecco
University of Notre Dame, Notre Dame, IN 46556, USA

J. R. G. Alsmiller, T. A. Gabriel, T. Handler
Oak Ridge National Laboratory, Oak Ridge, TN 37831, USA

J. Brau, R. Frey, M. Iwasaki, N. B. Sinev, D. Strom
University of Oregon, Eugene, OR 97403, USA

F. Colecchia, F. Dal Corso, A. Dorigo, F. Galeazzi, M. Margoni, G. Michelon, M. Morandin, M. Posocco, M. Rotondo, F. Simonetto, R. Stroili, E. Torassa, C. Voci
Università di Padova, Dipartimento di Fisica and INFN, I-35131 Padova, Italy

M. Benayoun, H. Briand, J. Chauveau, P. David, Ch. de la Vaissière, L. Del Buono, O. Hamon, F. Le Diberder, Ph. Leruste, J. Lory, L. Roos, J. Stark, S. Versillé
Universités Paris VI et VII, Lab de Physique Nucléaire H. E., F-75252 Paris, France

P. F. Manfredi, V. Re, V. Speziali
Università di Pavia, Dipartimento di Elettronica and INFN, I-27100 Pavia, Italy

E. D. Frank, L. Gladney, Q. H. Guo, J. H. Panetta
University of Pennsylvania, Philadelphia, PA 19104, USA

C. Angelini, G. Batignani, S. Bettarini, M. Bondioli, M. Carpinelli, F. Forti, M. A. Giorgi, A. Lusiani, F. Martinez-Vidal, M. Morganti, N. Neri, E. Paoloni, M. Rama, G. Rizzo, F. Sandrelli, G. Simi, G. Triggiani, J. Walsh
Università di Pisa, Scuola Normale Superiore and INFN, I-56010 Pisa, Italy

[3] Also with Università della Basilicata, I-85100 Potenza, Italy

M. Haire, D. Judd, K. Paick, L. Turnbull, D. E. Wagoner

Prairie View A&M University, Prairie View, TX 77446, USA

J. Albert, C. Bula, P. Elmer, C. Lu, K. T. McDonald, V. Miftakov, S. F. Schaffner, A. J. S. Smith, A. Tumanov, E. W. Varnes

Princeton University, Princeton, NJ 08544, USA

G. Cavoto, D. del Re, R. Faccini,[4] F. Ferrarotto, F. Ferroni, K. Fratini, E. Lamanna, E. Leonardi, M. A. Mazzoni, S. Morganti, G. Piredda, F. Safai Tehrani, M. Serra, C. Voena

Università di Roma La Sapienza, Dipartimento di Fisica and INFN, I-00185 Roma, Italy

S. Christ, R. Waldi

Universität Rostock, D-18051 Rostock, Germany

P. F. Jacques, M. Kalelkar, R. J. Plano

Rutgers University, New Brunswick, NJ 08903, USA

T. Adye, B. Franek, N. I. Geddes, G. P. Gopal, S. M. Xella

Rutherford Appleton Laboratory, Chilton, Didcot, Oxon, OX11 0QX, United Kingdom

R. Aleksan, G. De Domenico, S. Emery, A. Gaidot, S. F. Ganzhur, P.-F. Giraud, G. Hamel de Monchenault, W. Kozanecki, M. Langer, G. W. London, B. Mayer, B. Serfass, G. Vasseur, Ch. Yèche, M. Zito

DAPNIA, Commissariat à l'Energie Atomique/Saclay, F-91191 Gif-sur-Yvette, France

N. Copty, M. V. Purohit, H. Singh, F. X. Yumiceva

University of South Carolina, Columbia, SC 29208, USA

I. Adam, P. L. Anthony, D. Aston, K. Baird, J. P. Berger, E. Bloom, A. M. Boyarski, F. Bulos, G. Calderini, R. Claus, M. R. Convery, D. P. Coupal, D. H. Coward, J. Dorfan, M. Doser, W. Dunwoodie, R. C. Field, T. Glanzman, G. L. Godfrey, S. J. Gowdy, P. Grosso, T. Himel, T. Hryn'ova, M. E. Huffer, W. R. Innes, C. P. Jessop, M. H. Kelsey, P. Kim, M. L. Kocian, U. Langenegger, D. W. G. S. Leith, S. Luitz, V. Luth, H. L. Lynch, H. Marsiske, S. Menke, R. Messner, K. C. Moffeit, R. Mount, D. R. Muller, C. P. O'Grady, M. Perl, S. Petrak, H. Quinn, B. N. Ratcliff, S. H. Robertson, L. S. Rochester, A. Roodman, T. Schietinger, R. H. Schindler, J. Schwiening, V. V. Serbo, A. Snyder, A. Soha, S. M. Spanier, J. Stelzer, D. Su, M. K. Sullivan, H. A. Tanaka, J. Va'vra, S. R. Wagner, A. J. R. Weinstein, W. J. Wisniewski, D. H. Wright, C. C. Young

Stanford Linear Accelerator Center, Stanford, CA 94309, USA

P. R. Burchat, C. H. Cheng, D. Kirkby, T. I. Meyer, C. Roat

Stanford University, Stanford, CA 94305-4060, USA

R. Henderson

TRIUMF, Vancouver, BC, Canada V6T 2A3

W. Bugg, H. Cohn, A. W. Weidemann

University of Tennessee, Knoxville, TN 37996, USA

[4] Also with University of California at San Diego, La Jolla, CA 92093, USA

J. M. Izen, I. Kitayama, X. C. Lou, M. Turcotte
University of Texas at Dallas, Richardson, TX 75083, USA

F. Bianchi, M. Bona, B. Di Girolamo, D. Gamba, A. Smol, D. Zanin
Università di Torino, Dipartimento di Fisica Sperimentale and INFN, I-10125 Torino, Italy

L. Bosisio, G. Della Ricca, L. Lanceri, A. Pompili, P. Poropat, M. Prest, E. Vallazza, G. Vuagnin
Università di Trieste, Dipartimento di Fisica and INFN, I-34127 Trieste, Italy

R. S. Panvini
Vanderbilt University, Nashville, TN 37235, USA

C. M. Brown, A. De Silva, R. Kowalewski, J. M. Roney
University of Victoria, Victoria, BC, Canada V8W 3P6

H. R. Band, E. Charles, S. Dasu, F. Di Lodovico, A. M. Eichenbaum, H. Hu, J. R. Johnson, R. Liu, J. Nielsen, Y. Pan, R. Prepost, I. J. Scott, S. J. Sekula, J. H. von Wimmersperg-Toeller, S. L. Wu, Z. Yu, H. Zobernig
University of Wisconsin, Madison, WI 53706, USA

T. M. B. Kordich, H. Neal
Yale University, New Haven, CT 06511, USA

1 Introduction

In the Standard Model, $B^0\overline{B}^0$ [1] mixing occurs through second-order weak diagrams involving the exchange of up-type quarks, with the top quark contributing the dominant amplitude. A measurement of Δm_d, the difference between the mass eigenstates of the B^0–$\overline{B}^0$ system, is therefore sensitive to the magnitude of the Cabibbo-Kobayashi-Maskawa matrix [2] element V_{td}. At present the sensitivity to V_{td} is not limited by experimental precision on Δm_d, but by other uncertainties in the calculation, in particular the quantity $f_B^2 B_B$, where f_B is the B^0 decay constant, and B_B is the so-called bag factor, representing the strong interaction matrix elements.

The phenomenon of particle–anti-particle mixing in the neutral B meson system was first observed almost fifteen years ago [3]. The oscillation frequency has been extensively studied with both time-integrated and time-dependent techniques [4].

In this paper we present a measurement of time-dependent mixing based on a sample of $20.7\,\mathrm{fb}^{-1}$ of data recorded at the $\Upsilon(4S)$ resonance with the *BABAR* detector at the Stanford Linear Accelerator Center. At the PEP-II asymmetric-energy e^+e^- collider, resonant production of the $\Upsilon(4S)$ provides a copious source of $B^0\overline{B}^0$ pairs moving along the beam axis (z direction) with a Lorentz boost of $\beta\gamma = 0.56$. The typical separation between the two neutral B decay vertices is $\langle|\Delta z|\rangle \approx \beta\gamma c\tau_{B^0} = 260\,\mu\mathrm{m}$, where $\tau_{B^0} = 1.548 \pm 0.032\,\mathrm{ps}$ is the B^0 lifetime [4].

2 Analysis method

The $B^0\overline{B}^0$ mixing probability is a function of Δm_d and the time difference between the B decays, $\Delta t \simeq \Delta z/\beta\gamma c$:

$$\begin{aligned} Prob(B^0\overline{B}^0 \to B^0B^0, \overline{B}^0\overline{B}^0) &\propto \mathrm{e}^{-|\Delta t|/\tau_{B^0}}(1-\cos\Delta m_d\Delta t) \\ Prob(B^0\overline{B}^0 \to B^0\overline{B}^0) &\propto \mathrm{e}^{-|\Delta t|/\tau_{B^0}}(1+\cos\Delta m_d\Delta t) \end{aligned}$$

resulting in a time-dependent probability to observe *mixed*, B^0B^0 and $\overline{B}^0\overline{B}^0$, or *unmixed*, $B^0\overline{B}^0$, pairs produced in $\Upsilon(4S)$ decay. The effect can be measured by reconstructing one B in a flavor eigenstate, referred to as B_{rec}, while using the remaining particles from the decay of the other B, referred to as B_{tag}, to identify, or "tag", its flavor. The charges of identified leptons and kaons are the primary indicators, but other information in the event can also be used to identify the flavor of B_{tag}, resulting in a total of four non-overlapping tagging categories. The tagging algorithm used in this analysis is identical to that employed for *CP* violation studies, in which one B is fully reconstructed in a *CP* eigenstate [5].

If the flavor tagging were perfect, the asymmetry as a function of Δt

$$A_{mixing}(\Delta t) = \frac{N_{unmixed} - N_{mixed}}{N_{unmixed} + N_{mixed}}$$

would be a cosine with unit amplitude. However, the tagging algorithm incorrectly identifies the flavor of B_{tag} with a probability w_i for the i^{th} tagging category. This mistag rate reduces the amplitude of the oscillation by a factor $(1-2w_i)$. A simultaneous fit to the mixing frequency and its amplitude allows the determination of both Δm_d and the mistag rates, w_i.

Neglecting any background contributions, the probability density functions (PDFs) for the mixed (+) and unmixed (−) events, $\mathcal{H}_{\pm,sig}$, can be expressed as the convolution of the decay

distribution for the i^{th} tagging category

$$h_{\pm}(\Delta t;\Delta m_d,w_i)=\frac{\mathrm{e}^{-|\Delta t|/\tau_{B^0}}}{4\tau_{B^0}}\left[1\mp(1-2w_i)\cos\Delta m_d\Delta t\right],$$

with a time resolution function $\mathcal{R}(\Delta t-\Delta t_{true};\hat{a}_i)$,

$$\mathcal{H}_{\pm,sig}(\Delta t;\Delta m_d,w_i,\hat{a}_i)=h_{\pm}(\Delta t_{true};\Delta m_d,w_i)\otimes\mathcal{R}(\Delta t-\Delta t_{true};\hat{a}_i).$$

where $\hat{a}_i$ are the parameters of the resolution function. A log-likelihood function is then constructed from the sum of $\log\mathcal{H}_{\pm,sig}$ over all mixed and unmixed events, and over the different tagging categories.

The log-likelihood is maximized to extract the mixing parameter Δm_d and, simultaneously, the mistag rates, w_i. The correlation among these parameters is small, because the rate of mixed events at low values of Δt, where the $B^0\overline{B}^0$ mixing probability is small, is principally governed by the mistag rate. Conversely, the sensitivity to Δm_d increases at larger values of Δt; for Δt near twice the lifetime, half of the B^0 mesons will have oscillated.

3 The *BABAR* detector

The *BABAR* detector is a 4π charged and neutral spectrometer described in more detail elsewhere [6]. Charged particles are detected and their momenta measured by a combination of a 40-layer drift chamber (DCH) and a five-layer silicon vertex tracker (SVT) embedded in a 1.5-T solenoidal magnetic field. Decay vertices are typically reconstructed with a resolution along the boost direction of 65 μm for fully reconstructed B mesons. A ring imaging Cherenkov detector, the DIRC, is used for charged hadron identification. A finely segmented CsI(Tl) electromagnetic calorimeter (EMC) is used to detect photons and neutral hadrons, and also for electron identification. The iron flux return (IFR) is segmented and instrumented with multiple layers of resistive plate chambers for the identification of muons and long-lived neutral hadrons.

4 Event selection and B reconstruction

The analysis uses a sample of multihadron events, which are selected by demanding a minimum of three reconstructed charged tracks and a total charged and neutral energy greater than 4.5 GeV in the fiducial region of the detector, and a reconstructed event vertex within 0.5 cm of the measured interaction point [6] in the plane transverse to the beamline.

Electron candidates must satisfy a cut on the ratio of calorimeter energy to track momentum of $0.88<E/p<1.3$, a cluster shape consistent with an electromagnetic shower, and DCH $\mathrm{d}E/\mathrm{d}x$ and DIRC Cherenkov angle consistent with an electron.

Muon candidates must satisfy requirements on the number of interaction lengths of IFR iron penetrated of $N_\lambda>2.2$, on the difference in the measured and expected interaction lengths penetrated of $N_\lambda^{exp}-N_\lambda<1$, on the position match between the extrapolated DCH track and the IFR hits, and on the average and spread of the number of IFR hits per layer.

Pairs of photons in the EMC with energy above 30 MeV are constrained to the known π^0 mass if they are within $\pm20\,\mathrm{MeV}/c^2$ of the nominal invariant mass [4], and their summed energy is greater than 200 MeV.

$K^0_S \to \pi^+\pi^-$ candidates are required to have an invariant mass between 462 and 534 MeV/c^2, and a χ^2 probability for the vertex fit of greater than 0.1%. The transverse flight distance of the K^0_S candidate from the primary event vertex must be greater than 2 mm.

$\overline{D}^0$ candidates are identified in the decays channels $K^+\pi^-$, $K^+\pi^-\pi^0$, $K^+\pi^+\pi^-\pi^-$ and $K^0_S\pi^+\pi^-$. D^- candidates are selected in the $K^+\pi^-\pi^-$ and $K^0_S\pi^-$ modes. Kaons from D^- decays and charged daughters from $\overline{D}^0 \to K^+\ \pi^-$ are required to have a momentum greater than 200 MeV/c. All other charged $\overline{D}$ daughters are required to have a momentum greater than 150 MeV/c. For $\overline{D}^0 \to K^+\pi^-\pi^0$, we only reconstruct the dominant resonant mode $\overline{D}^0 \to K^+\rho^-$, followed by $\rho^- \to \pi^-\pi^0$. The $\pi^-\pi^0$ mass is required to lie within ± 150 MeV/c^2 of the nominal ρ mass [4] and the angle between the π^- and $\overline{D}^0$ in the ρ rest frame, $\theta^*_{D^0\pi}$, must satisfy $|\cos\theta^*_{D^0\pi}| > 0.4$. $\overline{D}^0$ and D^- candidates are required to have momentum greater than 1.3 GeV/c in the $\Upsilon(4S)$ frame, an invariant mass within $\pm 3\sigma$ of the nominal value [4] and a χ^2 probability of the topological vertex fit greater than 0.1%. A mass constraint is applied to selected $\overline{D}^0$ candidates.

D^{*-} candidates are formed by combining a $\overline{D}^0$ and a pion with momentum less than 450 MeV/c. The soft pion is constrained to originate from the beamspot when the D^{*-} vertex is computed. Those D^{*-} candidates with $m(\overline{D}^0\pi^-) - m(\overline{D}^0)$ lying within $\pm 2.5\sigma$ of the nominal value [4] are selected, where $\sigma = 1.1$ MeV/c^2 for $\overline{D}^0 \to K^+\pi^-\pi^0$ mode and 0.8 MeV/c^2 for all other modes.

$J/\psi \to e^+e^-$ or $\mu^+\mu^-$ candidates must have at least one decay product positively identified as an electron or muon. Electron candidates outside the calorimeter acceptance must have DCH $\mathrm{d}E/\mathrm{d}x$ information consistent with that for an electron. The second muon candidate, if within the acceptance of the calorimeter, must be consistent with being a minimum ionizing particle. J/ψ candidates are required to lie in the invariant mass interval 2.95 (3.06) to 3.14 GeV/c^2 for the e^+e^- ($\mu^+\mu^-$) channel.

B^0 candidates in the flavor eigenstate decay modes $D^{(*)-}\pi^+/\rho^+/a_1^+$ are formed by combining a D^{*-} or D^- candidate with a π^+, ρ^+ ($\rho^+ \to \pi^+\pi^0$) or a_1^+ ($a_1^+ \to \pi^+\pi^-\pi^+$); likewise $B^0 \to J/\psi K^{*0}$ candidates are reconstructed from combinations of J/ψ candidates with a K^{*0} ($K^{*0} \to K^+\pi^-$).

For $B^0 \to D^{*-}\rho^+$, the π^0 from the ρ^+ decay is required to have an energy greater than 300 MeV. For $B^0 \to D^{*-}a_1^+$, the a_1^+ is reconstructed by combining three charged pions, with invariant mass in the range 1.0 to 1.6 GeV/c^2 and a χ^2 probability of the vertex fit of the a_1^+ candidate of greater than 0.1%. For most B^0 modes, no particle identification or only a loose requirement is enough to achieve reasonable signal purities.

Continuum background is rejected by requiring the normalized second Fox-Wolfram moment [7] be less than 0.5. Further suppression is achieved by a mode-dependent restriction on the angle, θ_{th}, between the thrust axes of decay products from B_{rec} and B_{tag} respectively in the $\Upsilon(4S)$ frame.

B^0 candidates are identified with the difference ΔE between the energy of the candidate and the beam energy $E^{\rm cm}_{\rm beam}$ in the center-of-mass frame and the beam-energy substituted mass $m_{\rm ES} = \sqrt{(E^{\rm cm}_{\rm beam})^2 - (p^{\rm cm}_B)^2}$. Those candidates with $m_{\rm ES} > 5.2$ MeV/c^2 and $\Delta E = 0$ within ± 2.5 standard deviations (typically $|\Delta E| < 40$ MeV) are selected. If there is more than one candidate satisfying these conditions only the one with the smallest ΔE is retained. Finally, a topological vertex fit of the candidate must converge.

5 Decay time difference determination

The decay time difference, Δt, between B decays is determined from the measured separation along the z axis between the reconstructed $B = B_{rec}$ and flavor-tagging decay $B = B_{tag}$ vertices $\Delta z = z_{rec} - z_{tag}$. This Δz is then converted into Δt using the known $\Upsilon(4S)$ boost and correcting

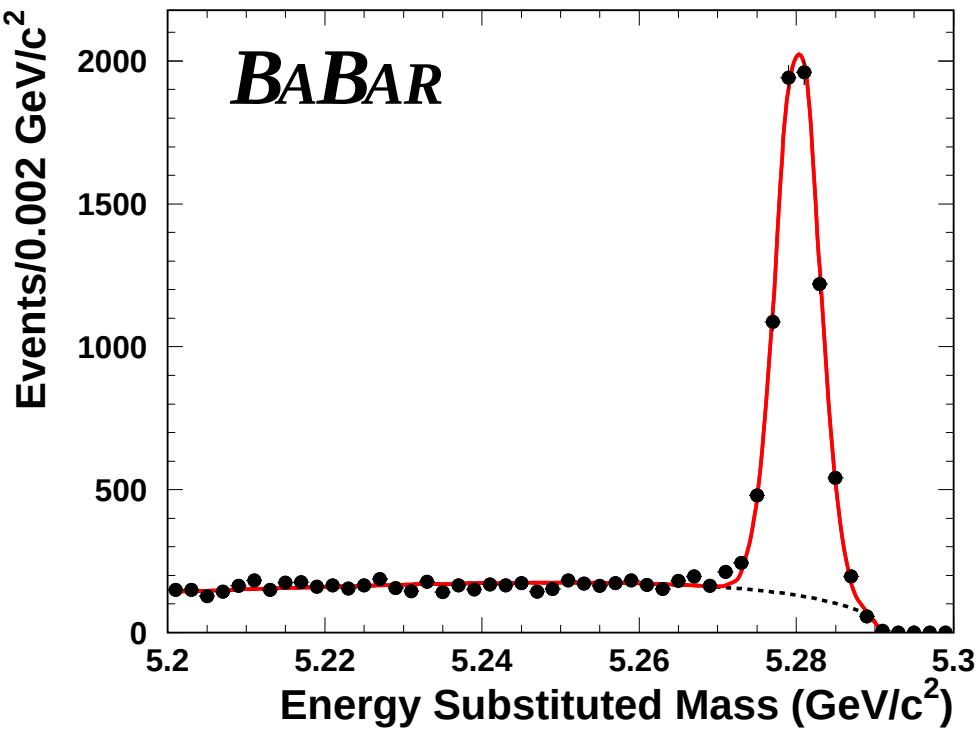

Figure 1: Distribution of $m_{\rm ES}$ for all B^0 hadronic candidates decaying into flavor eigenstate modes.

on an event-by-event basis for the direction of the B mesons with respect to the z direction in the $\Upsilon(4S)$ frame. The resolution of the Δt measurement is dominated by the z resolution of the tagging vertex. The B_{tag} decay vertex uses all tracks in the event except those incorporated in B_{rec}. An additional constraint is provided by including a calculated B_{tag} production point and three-momentum, determined from the three momentum of the B_{rec} candidate, its decay vertex, and the average position of the interaction point and the $\Upsilon(4S)$ boost. Reconstructed K^0_S or Λ candidates are used as input to the fit in place of their daughters in order to reduce bias due to long-lived particles. Tracks with a large contribution to the χ^2 are iteratively removed from the fit, until all remaining tracks have a reasonable fit probability or all tracks are removed. Only those candidates with $|\Delta z| < 3.0\,{\rm mm}$ and $\sigma_{\Delta z} < 400\,\mu{\rm m}$ are retained. The distribution of $m_{\rm ES}$ for the surviving candidates is shown in Fig. 1 along with a fit with a Gaussian distribution for the signal and the ARGUS function [8] for the background. At this point the sample contains 6662 ± 93 signal events, with a purity, defined in the region $m_{\rm ES} > 5.27\,{\rm GeV}/c^2$, that varies between 80–95% depending on the B^0 decay mode.

In the likelihood, the time resolution function can be approximated by a sum of three Gaussian distributions with different means and widths,

$$\mathcal{R}(\Delta t;\hat{a}_i) = \sum_{k=1}^{3} \frac{f_k}{\sigma_k\sqrt{2\pi}} {\rm e}^{-(\Delta t - \Delta t_{true} - \delta_{k,i})^2/2{\sigma_k}^2},$$

where, for the core and tail Gaussians, the widths $\sigma_{1,2} = S_{1,2} \times \sigma_{\Delta t}$ are the scaled event-by-event

measurement error, $\sigma_{\Delta t}$, derived from the vertex fits. The third Gaussian, with a fixed width of $\sigma_3 = 8\,\text{ps}$, accounts for less than 1% of outlier events with incorrectly reconstructed vertices. A separate core bias, $\delta_{1,i}$, is allowed for each tagging category i to account for small shifts due to inclusion of charm decay products in the tag vertex, while a common bias δ_2 is used for the tail component. The tail and outlier fractions and the scale factors are assumed to be the same for all decay modes, since the precision of the B_{tag} vertex dominates Δt. This assumption is confirmed by Monte Carlo simulation studies.

6 Flavor tagging

After the daughter tracks of the reconstructed B are removed, the remaining tracks are analyzed to determine the flavor of the B_{tag}, and this ensemble is assigned a tag flavor, either B^0 or $\overline{B}^0$. For this purpose, we use the flavor tagging information carried by primary leptons from semileptonic B decays, charged kaons, soft pions from D^* decays, and more generally by high momentum charged particles to uniquely assign each event to a tagging category. The effective tagging efficiency $Q_i = \varepsilon_i(1-2w_i)^2$, where ε_i is the fraction of events assigned to category i, is used as the basis for optimization of category selection criteria. The statistical error on Δm_d is proportional to $1/\sqrt{Q}$, where $Q = \sum Q_i$.

Events are assigned to the `Lepton` category if they contain an identified lepton with a center-of-mass momentum greater than 1.0 or 1.1 GeV/c for electrons and muons, respectively. The momentum requirement selects mostly primary leptons by suppressing opposite-sign leptons from semileptonic charm decays.

Kaons are identified with a neural network based on the likelihood ratios in the SVT and DCH, derived from $\mathrm{d}E/\mathrm{d}x$ measurements, and in the DIRC, calculated by comparing individual photomultiplier hits with the expected pattern of Cherenkov light for either kaons or pions. The charges of all identified kaons are summed, and if $\sum Q_K \neq 0$ the event is assigned to the `Kaon` category.

The final two categories involve a multivariable analysis using a neural network, which is trained to identify primary leptons, kaons, and soft pions, and the momentum and charge of the track with the maximum center-of-mass momentum. Depending on the value of the output variable from the neural net, events are given a B^0 or $\overline{B}^0$ tag and assigned to the mutually exclusive categories `NT1` (more certain tags) or `NT2` (less certain tags). About 30% of all events are assigned to no tagging category and are excluded from the analysis.

Tagging assignments for events are made mutually exclusive by the hierachical use of the tagging categories. Events with a `Lepton` tag and no conflicting `Kaon` tag use the `Lepton` category. If no `Lepton` tag exists, then the `Kaon` category is used, if a tag exists. Otherwise the two neural network categories are used. The number of tagged events per category is given in Table 1. In total, there are 4538 ± 75 tagged signal events.

7 Background PDF

In the presence of backgrounds, the probability distribution functions $\mathcal{H}_{\pm,sig}$ must be extended to include a term for each significant background source, which are allowed to differ for each tagging

Table 1: Event yields for the different tagging categories used in this analysis, as obtained from fits to the $m_{\rm ES}$ distributions after all selection requirements. The purity is quoted for $m_{\rm ES} > 5.270\,{\rm MeV}/c^2$.

Category	Tagged	Efficiency (%)	Purity (%)
`Lepton`	754 ± 28	11.3 ± 0.4	97.1 ± 0.6
`Kaon`	2317 ± 54	34.8 ± 0.6	85.2 ± 0.8
`NT1`	556 ± 26	8.3 ± 0.3	88.7 ± 1.5
`NT2`	910 ± 36	13.7 ± 0.4	83.0 ± 1.3
Total	4538 ± 75	68.1 ± 0.9	86.7 ± 0.5

category:

$$\mathcal{H}_{\pm,i} = f_{i,sig}\mathcal{H}_{\pm,sig} + \sum_{k=bkgd} f_{i,k}\mathcal{B}_{\pm,i,k}(\Delta t; \hat{b}_{\pm,i,k})$$

where the background PDFs, $\mathcal{B}_{\pm,i,k}$, provide an empirical description for the Δt distribution of the background events in the sample. The fraction of background events for each source and tagging category is given by $f_{i,k}$, while $\hat{b}_{\pm,i,k}$ are parameters used to characterize each source of background by tagging category for mixed and unmixed events.

The probability that a B^0 candidate is a signal or a background event is determined from a separate fit to the observed $m_{\rm ES}$ distributions of B_{rec} candidates in each of the four tagging categories. We describe the $m_{\rm ES}$ shape with a single Gaussian distribution $\mathcal{S}(m_{\rm ES})$ for the signal and an ARGUS parameterization $\mathcal{A}(m_{\rm ES})$ for the background. Based on this fit, the event-by-event signal probabilities $f_{sig,i}$ are given by

$$f_{i,{\rm sig}}(m_{\rm ES}) = \frac{\mathcal{S}(m_{\rm ES})}{\mathcal{S}(m_{\rm ES}) + \mathcal{A}(m_{\rm ES})}$$

The sum of signal and background fractions is forced to unity.

The Δt distributions of the combinatorial background are assumed to be described with a zero lifetime component and a non-oscillatory component with non-zero lifetime. We fit for separate resolution function parameters for the signal and the background in order to minimize correlations of the time structure between background and signal. Candidates with low signal probability, *i.e.,* in the $m_{\rm ES}$ sideband region below $5.27\,{\rm GeV}/c^2$, dominate the determination of these background parameters.

8 Extraction of Δm_d

The value of Δm_d is extracted from the tagged flavor-eigenstate B^0 sample with an unbinned maximum likelihood fit involving a total of 34 parameters, including Δm_d. The value of Δm_d was kept hidden throughout the analysis until the systematic errors were finalized, in order to eliminate possible experimenter's bias.

The results from the likelihood fit to the tagged B^0 sample are summarized in Table 2. The probability of obtaining a likelihood smaller than the one observed is determined to be 28% from a

Table 2: Results from the likelihood fit to the Δt distributions of the tagged hadronic B^0 decays. Δm_d and the mistag rates include small corrections corresponding to the difference between the generated and reconstructed values in simulated signal events.

Parameter	Value	Parameter	Value
Δm_d ($\hbar\,\mathrm{ps}^{-1}$)	0.519 ± 0.020	$\delta_{1,\mathtt{Lepton}}$(ps)	$+0.11 \pm 0.07$
$w_{\mathtt{Lepton}}$	0.085 ± 0.018	$\delta_{1,\mathtt{Kaon}}$(ps)	-0.20 ± 0.05
$w_{\mathtt{Kaon}}$	0.167 ± 0.014	$\delta_{1,\mathtt{NT1}}$(ps)	$+0.01 \pm 0.09$
$w_{\mathtt{NT1}}$	0.195 ± 0.026	$\delta_{1,\mathtt{NT2}}$(ps)	-0.20 ± 0.08
$w_{\mathtt{NT2}}$	0.326 ± 0.024	δ_2(ps)	$-1.2^{+0.9}_{-1.6}$
S_1	$1.42^{+0.08}_{-0.09}$	f_2	$0.032^{+0.03}_{-0.02}$
S_2	$5.5^{+2.0}_{-1.6}$	f_3	0.001 ± 0.004

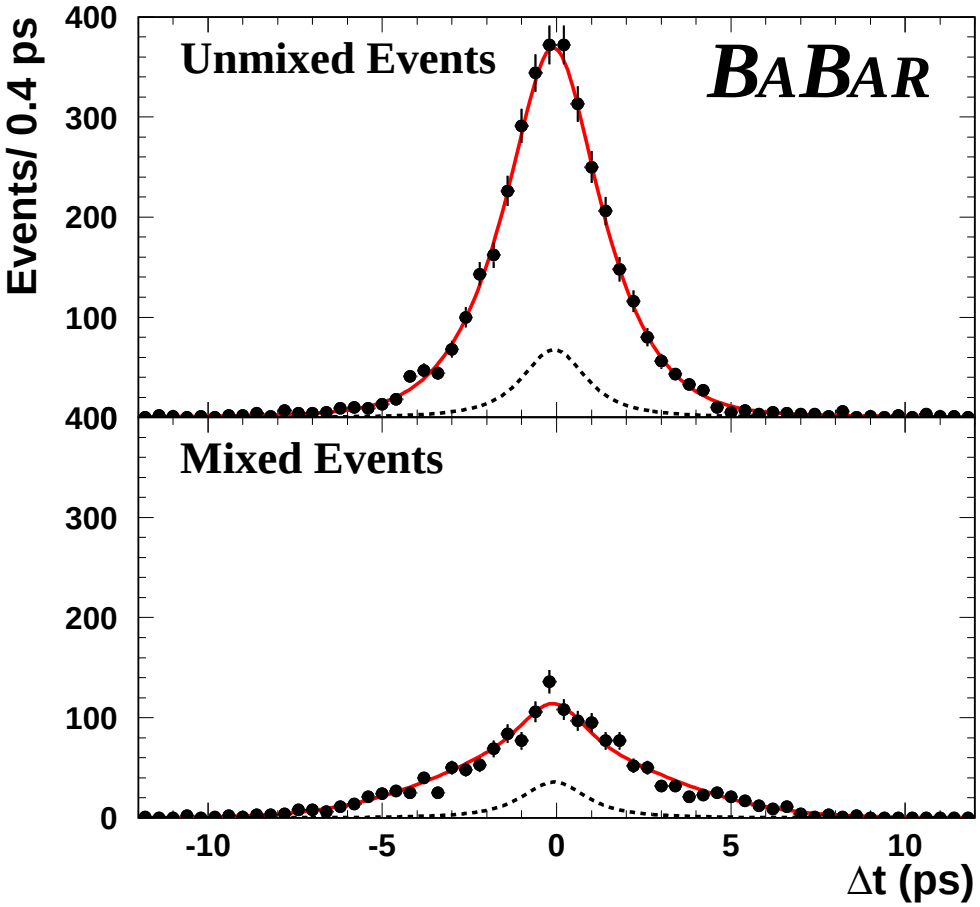

Figure 2: Δt distributions in data for the selected mixed and unmixed tagged hadronic B^0 decays ($m_{\mathrm{ES}} > 5.27\,\mathrm{GeV}/c^2$), with overlaid the projection of the likelihood fit. The background contribution is indicated by the dashed curve.

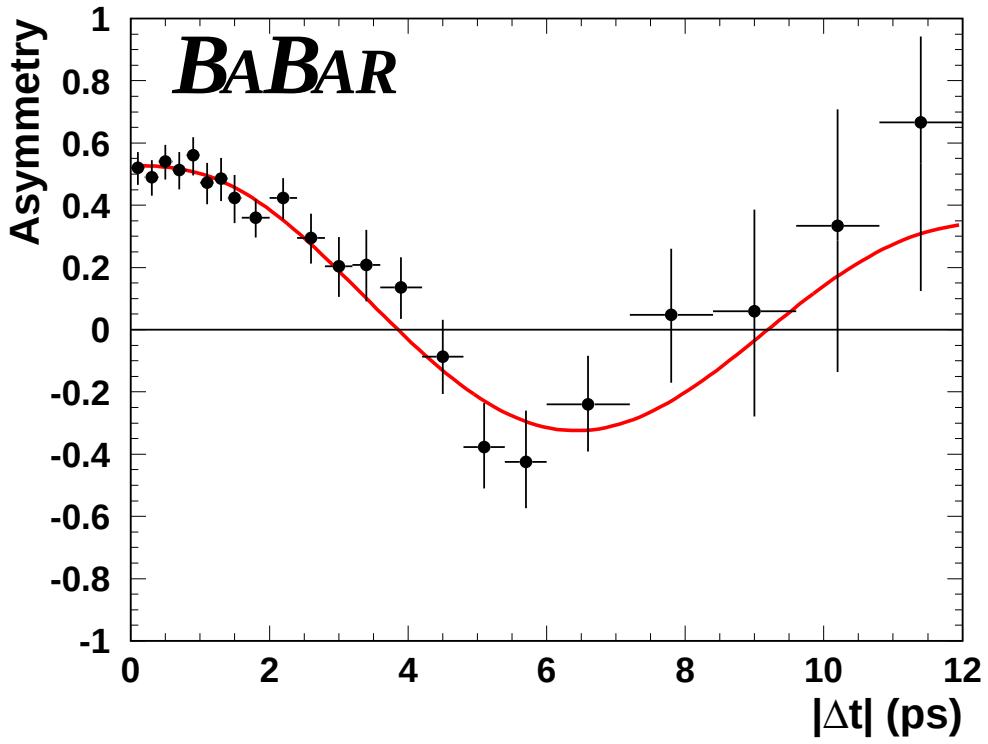

Figure 3: The time-dependent asymmetry $\mathcal{A}_{mix}(\Delta t)$ between unmixed and mixed events as a function of $|\Delta t|$.

large number of simulated experiments, each generated according to the parameters obtained from the fit. The measured value for Δm_d is:

$$\Delta m_d = 0.519 \pm 0.020(stat) \pm 0.016(syst)\,\hbar\,\mathrm{ps}^{-1}.$$

where the sources of systematic error are discussed below. The observed distribution of mixed and unmixed events and the asymmetry, $\mathcal{A}_{mix}$ are shown in Fig. 2 and 3 as a function of Δt along with projections of the likelihood fit result.

9 Systematic studies and cross checks

The conversion of Δz to Δt introduces a systematic uncertainty ($\pm 0.007\,\hbar\,\mathrm{ps}^{-1}$) due to the limited knowledge of the PEP-II boost, the z length scale of *BABAR* (determined from secondary interactions in a beam pipe section of known length) and the $B_{\rm rec}$ momentum vector in the $\Upsilon(4S)$ frame.

The signal Δt resolution parameters are determined directly from data by the fit, contributing ± 0.006 in quadrature to the statistical error. Residual uncertainties ($\pm 0.005\,\hbar\,\mathrm{ps}^{-1}$), are attributed to the choice of the parameterization, its description of the outliers, and the capability of the resolution model to deal with various plausible misalignment scenarios applied to the Monte Carlo simulation.

The parameters of the background Δt distribution are left free in the likelihood fit, but systematic errors ($\pm 0.005\,\hbar\,\mathrm{ps}^{-1}$), are introduced by the residual uncertainty from the $m_{\rm ES}$ fit used

to determine the signal probability, the assumed parameterization of the background Δt distributions and resolution function, and the small amount of correlated B^+ background remaining in the sample.

Finally, statistical limitations of Monte Carlo validation tests ($\pm 0.004\,\hbar\,\mathrm{ps}^{-1}$), the full size of a (negative) correction obtained from Monte Carlo ($\pm 0.009\,\hbar\,\mathrm{ps}^{-1}$), and the variation of the fixed B^0 lifetime (due to its negative correlation with Δm_d) within known errors [4] ($\pm 0.006\,\hbar\,\mathrm{ps}^{-1}$) contribute. A summary of these sources of systematic error for the hadronic B^0 sample is shown in Tables 3.

Various checks on the consistency of the result were performed by splitting the data in sub-samples according to several key variables, including (but not limited to) the decay modes of B_{rec}, the tagging category of B_{tag}, and the flavor of either B_{rec} or B_{tag}. The value of Δm_d was found to be consistent for all sub-samples.

Table 3: Systematic uncertainties for Δm_d.

Source	$\delta\Delta m_d$ [$\hbar$ ps^{-1}]
Beamspot	
position and size	0.001
Δz to Δt conversion	
PEP-II boost	0.003
z scale	< 0.005
method	0.004
Δt resolution	
outliers	0.002
parameterization	0.003
SVT alignment	0.004
Backgrounds	
Δt model	0.001
Resolution parameterization	0.003
Fractions	0.003
Correlated	0.002
Monte Carlo	
statistics	0.004
correction	0.009
B^0 lifetime	0.006
Total Systematic Error	0.016

10 Summary

We have measured the value for Δm_d to be:

$$\Delta m_d = 0.519 \pm 0.020(stat) \pm 0.016(syst)\,\hbar\,\mathrm{ps}^{-1}.$$

This result is one of the best single measurements available and is consistent with the current world average [4]. Moreover, the error on Δm_d is still dominated by the statistical size of the reconstructed

B^0 sample, leaving substantial room for further improvement as more data is accumulated at *BABAR*. The measurement shares the same flavor-eigenstate sample as used for the determination of sin2β. Thus, it provides an essential validation for the reported sin2β result [5] and, in particular, the mistag rates that appear as coefficients of the mixing asymmetry.

11 Acknowledgments

We are grateful for the extraordinary contributions of our PEP-II colleagues in achieving the excellent luminosity and machine conditions that have made this work possible. The collaborating institutions wish to thank SLAC for its support and the kind hospitality extended to them. This work is supported by the US Department of Energy and National Science Foundation, the Natural Sciences and Engineering Research Council (Canada), Institute of High Energy Physics (China), the Commissariat à l'Energie Atomique and Institut National de Physique Nucléaire et de Physique des Particules (France), the Bundesministerium für Bildung und Forschung (Germany), the Istituto Nazionale di Fisica Nucleare (Italy), the Research Council of Norway, the Ministry of Science and Technology of the Russian Federation, and the Particle Physics and Astronomy Research Council (United Kingdom). Individuals have received support from the Swiss National Science Foundation, the A. P. Sloan Foundation, the Research Corporation, and the Alexander von Humboldt Foundation.

References

[1] The symbol B^0 refers to the B_d meson; charge conjugate modes are implied throughout this paper.

[2] N. Cabibbo, Phys. Lett. **10**, 531 (1963); M. Kobayashi and T. Maskawa, Prog. Theor. Phys. **49**, 652 (1973).

[3] UA1 Collab., C. Albajar *et al.*, Phys. Lett. **B186**, 247 (1987); ARGUS Collab., H. Albrecht *et al.*, Phys. Lett. **B192**, 245 (1987).

[4] D.E. Groom, *et al.*, Eur. Phys. Jour. C **15**, 1 (2000).

[5] *BABAR* Collab., B. Aubert *et al.*, Phys. Rev. Lett. **86**, 2515 (2001).

[6] *BABAR* Collab., B. Aubert *et al.*, *BABAR*-PUB-01/08, to appear in Nucl. Instr. and Methods

[7] G. C. Fox and S. Wolfram, Phys. Rev. Lett. **41**, 1581 (1978).

[8] ARGUS Collab., H. Albrecht *et al.*, Phys. Lett. **B185**, 218 (1987).